# Atmospheric Patterns over the Antarctic Peninsula

**Sergi Gonzalez[1,2]\*, Francisco Vasallo[1], Cayetana Recio-Blitz[3], José A. Guijarro[4], Jesús Riesco[1]**

[1]AEMET Antarctic Group, Spanish Meteorological Service (AEMET), Spain

[2]Department of Applied Physics, University of Barcelona, Spain

[3]Departmento de Matematica Aplicada a las TIC, Polytechnic University of Madrid, Spain

[4]Mediterranean Study Group, Spanish Meteorological Service (AEMET), Spain

Correspondence to:

S. Gonzalez, Territorial Delegation in Catalonia, AEMET. C/ Arquitecte Sert, 1, E-08003,

Barcelona, Spain. E-mail: sgonzalezh@aemet.es

## 1 Abstract

2        Using clustering analysis for the SLP field of the ERA Interim reanalysis between 1979 and

3    2016, five synoptic pressure patterns have been obtained for Drake area and Antarctic Peninsula (AP)

4    region (45ºS 75ºS 20ºW 120ºW). The five patterns have been named according their most important

5    features as *Low over the Wedell Sea* (LWS), *Low over the Amundsen and Bellingshausen Seas* (LAB),

6    *Low over the Drake Passage* (LDP), *Zonal over the Drake Passage* (ZDP) and *Ridge over the*

7    *Antarctic Peninsula* (RAP). Each atmospheric pattern has been described after analyzing their

8    development and evolution. A frequency analysis shows that the 5 atmospheric patterns present a

9    similar annual frequency but a large seasonal variability. Their transitions from one to other pattern

10   tends to follow a cycle in which synoptic atmospheric waves displaces eastwards a quarter-

11  wavelength. Four of the five atmospheric patterns (except RAP) are very influenced by ENSO and

12  SAM, specially LAB and LWS. Occurrence of LAB pattern presents a positive trend showing

1

agreement with other studies that indicates an enhancement of the Amundsen-Bellingshausen Sea Low. Finally, atmospheric circulation patterns have been related with the airmass advection and precipitation in Livingston Island showing the potential application to study the changes in the surface mass balance on the AP cryosphere.

**Key words:** South Shetland Islands, Antarctic Peninsula, South Shetland Islands, atmospheric patterns, climatology, Antarctica

## 1. Introduction

Ice mass lost by mountain glaciers and island ice caps is one of the major contributor to sea level rise (IPCC 2013). Compared to the large ice sheets, thermal and dynamic response of these ice masses are quicker, so they are more vulnerable to the global warming. Most ice caps are located on islands around the Antarctic Peninsula (AP) (Bliss et al. 2013) and many studies have shown evidence of their acceleration and thinning (i. e. Hock et al. 2009; Radić and Hock 2010, 2011; Gardner et al. 2013).

Ice cap thinning occurs as a response of the changing conditions in the AP region. The AP has warmed +3.7 ºC/century during the second half of 20th century (Vaughan et al. 2003), and although there has been a significant cooling between 1998 and 2015 (Carrasco 2013; Oliva et al. 2017), Turner et al. (2016) demonstrated that this period is consistent with the natural variability of the region, since it is affected by long-term persistence (Ludescher et al. 2016). Indeed, the AP region is characterized by a large interannual variability and its temperature is very sensitive to the state of both the El Niño-Southern Oscillation (ENSO) (Fogt and Bromwich 2006; Fogt et al. 2011; Clem and Fogt 2013) and the Southern Annular Mode (SAM) (Thompson and Solomon 2002; Van Den Broeke and Van Lipzig 2003; Marshall 2003). It has been shown that these climatological modes of variability modify the main climatic patterns in Antarctica (i. e. Amundsen-Bellingshausen Seas Low (ABSL), jet streams, etc.), suggesting that their change may be closely linked to synoptic pressure patterns (Carleton 2003).

Synoptic scale systems eventually determine the temperature and the moisture of the airmass

2

39     that contribute to the surface mass balance of the ice caps in the AP. Therefore, a further

40     understanding of the synoptic climatology and its relationship with other climatological parameters

41     may contribute to interpret the changes in the AP cryosphere.

42        Although the AP climatology has been extensively studied, only few studies have addressed

43     the synoptic climatology and its classification. Kejna (1993) used low-level analysis in the AP region

44     between 1986 and 1989 to make a classification according the air mass advection to H. Arctowski

45     Station in King George island. Govorukha and Timofeyev (2002) made a visual analysis with a set

46     of synoptic charts, satellite imagery and other operational information during three years between

47     1997 and 2000 to describe the main synoptic processes over the AP. Turner et al. (1998) examined

48     satellite imagery and operational data to analyze synoptic-scale low pressure systems in the AP region

49     during a year, classifying them according to the environment in which cyclogenesis took place.

50        These studies have contributed to improve the knowledge of the synoptic activity in the AP

51     region, but until now, no one has conducted an objective synoptic classification during an extended

52     period of time and using clustering techniques. This classification is addressed in this paper. Datasets

53     and the methodology used are detailed in Chapter 2. In Chapter 3 synoptic classification is described,

54     with an analysis of the trends and the relationship between the synoptic patterns found and different

55     modes of variability. In Chapter 4 we conduct an analysis comparing the synoptic patterns with the

56     air mass advected over Livingston island, discussing the possible effects on the surface mass balance

57     on the island glaciers. In chapter 5 we draw some conclusions. Recently, Cohen et al. (2013)

58     developed the objective synoptic classification for the Ross Sea region using the NCEP reanalysis.

59     This study may be considered as its natural extension to the AP region.

## 2. Datasets and methodology
### a) Cluster analysis

62        To obtain the synoptic pressure patterns in Drake area, we selected the mean sea level pressure

63     (SLP) field of the ERA Interim reanalysis (Dee et al. 2011). ERA Interim has been stated as one of

64     the most realistic reanalysis to describe the SLP and geopotential height at 500 hPa in Antarctic region

65     (Bracegirdle and Marshall 2012). The area selected was 45ºS 75ºS 20ºW 120ºW (Figure 1a), and is

66  wide enough to represent the climate patterns in the surroundings of Drake area and the AP. This area

67  may include few points located at high altitude in the Andean Mountains (South America) and

68  Eternity Range (Antarctic Peninsula), that are not expected to affect the cluster analysis. By contrast,

69  we carefully selected the area to not cover the Antarctic Plateau, an area with widespread high

70  altitudes where SLP reduction is not valid. The period analyzed ranges from 1 Jan 1979 until 31 Dec

71  2016. For each day, we employed the 12 UTC field as the SLP field that better represent the daily

72  synoptic pattern to compare with mean daily values of the automatic weather station (AWS) [see

73  Section 2c].

74      The approach we used for clustering was similar to that used by Cohen et al. (2013). Prior to

75  clustering we detrended the data by removing the mean SLP and weighted each data point by the

76  square root of latitude. Thereafter, we retrieved the atmospheric patterns using the *k-means* cluster

77  algorithm. This algorithm has been successfully used to do a cluster analysis in other regions (e. g.

78  Lana et al. 2007; Houssos et al. 2008; Cohen et al. 2013) and consists in minimizing the average

79  squared distance between all points in the same cluster to identify the centers of the cells. Single *k-

80  means* algorithm is very sensitive to the initial values and may give unsatisfactory solutions by

81  achieving local minimums. Thus, we improved the seeding algorithm employing the *k-means++*

82  method (Arthur and Vassilvitskii 2007) to guarantee to find optimal solutions. This methodology was

83  performed for K from 3 to 15 and repeated 10 times for each K to ensure the reproducibility (with

84  this methodology the 10 cluster fields obtained for each K were almost identical). As in Cohen et al.

85  2013, the final K set was selected by visual inspection of the center fields according to the expertise

86  of Antarctic AEMET forecasters in the area, selecting K5 as the one that best reproduce the synoptic

87  patterns of the AP area. The same procedure was also employed with the 500 hPa geopotential height

88  fields obtaining a similar set of clusters for K5.

89  b) Climate Indices

90      In order to evaluate the climatological variability of the synoptic patterns retrieved, they were

91  compared with two main climate modes of variability linked to the AP climate: Southern Annular

92  Mode (SAM) and El Niño Southern Oscillation (ENSO).

93    SAM is the principal mode of variability of the southern hemisphere circulation and its

94    changes has a large impact in the AP climate (Marshall et al. 2006). Surface temperatures over AP

95    have been linked to the strengthening or weakening of circumpolar westerlies associated to the SAM

96    (Thompson and Solomon 2002; van den Broeke and van Lipzig 2003; Marshall et al. 2006). Monthly

97    station-based SAM index calculated by Marshall (2003) [available on-line at

98    https://legacy.bas.ac.uk/met/gjma/sam.html] was used. This index is based on the zonal pressure

99    difference between 40°S and 65°S calculated using 12 stations, and it extends back until 1957.

100    Variability in the AP temperatures has been also associated with the phase of ENSO by

101    modulating the depth and the extension of the ABSL. We selected El Niño 3.4 index calculated from

102    HadlSST1 dataset (Rayner et al. 2003) [available on-line at

103    https://www.esrl.noaa.gov/psd/gcos_wgsp/Timeseries/Nino34/] as an index representative of the

104    ENSO state (Bamston et al. 1997).

105    c) Station based data
106    In Section 4, we compare the synoptic patterns with the distribution of daily mean

107    temperature, relative humidity and accumulated precipitation observed to study the air masses

108    advected over the AP. Data from the Spanish Base Juan Carlos I AWS (JCI, 62.66°S 60.39°W) (Bañon

109    and Vasallo 2015) in Livingston Island (South Shetland Islands) have been used to analyze the air

110    mass advected to the South Shetland Islands for each synoptic type (Figure 1b). A dataset of mean

111    daily values of temperature, relative humidity and precipitation accumulated from 2005 to 2016 was

112    obtained if at least 80% of the daily 10-minutes values were available. To standardize the observations

113    and fill the gaps the dataset has been homogenized against the daily values in another AWS located

114    at Gabriel de Castilla Station (GdC, 62.98°S 60.68°W) in Deception Island, and the surrounding grid

115    points of ERA Interim reanalysis (4 points located at the intersections between 62.25°S 60.75°W

116    63.00°S 60.00°W) (Figure 1b). The homogenization was performed by means of the R package

117    Climatol (Guijarro 2017), applied on the monthly aggregates to improve the break-point detection.

118    Two significant break-points were detected in the JCI temperature series, and three in GdC. The dates

119    of the break-points were refined with the aid of the meta-data of the stations before adjusting their

120   daily series. The same procedure was applied to the relative humidity (one break-point in JCI and two

121   in GdC) and precipitation (one break-point in JCI) series. Finally, the monthly means were subtracted

122   from daily means to obtain daily anomalies to compare them with the atmospheric patterns retrieved.


## 123   3. Synoptic Patterns in Maritime Antarctica

### 124   a) Description of synoptic patterns

125         Figure 2 shows the five SLP synoptic patterns (the centroid of each cluster) calculated between

126   1979 and 2016 from ERA Interim reanalysis. Besides evaluating the centroids, we considered to

127   analyze each pattern by examining some individual days (about 10 for each one) using Integrated

128   Data Viewer (UCAR/Unidata) software. Figure 3 presents some examples of synoptic maps and their

129   classification. For clarity, each cluster has been named according to the most important feature

130   presented as follows:

131   *Low over the Weddell Sea (LWS)*

132         This cluster shows the presence of a low east of Weddell Sea, produced either from the

133   maxima of cyclogenesis located in the southern part of the Weddell Sea (Simmonds and Keay 2000),

134   or from a low crossing the Drake Passage to the east. As a counterpoint, there is a presence of the

135   South Pacific subtropical anticyclone extending to the south east to the Bellingshausen Sea,

136   sometimes even coupling with the Continental Antarctic Anticyclone. This pattern presents an intense

137   meridian circulation from the south or southwest over the Antarctic Peninsula.

138   *Low over the Amundsen and Bellingshausen Seas (LAB)*

139         This cluster is characterized by the semi-permanent ABSL located around 100º W at the

140   easternmost climatological extension (Turner et al. 2013; Hosking et al. 2013; Raphael et al. 2016).

141   This pattern is composed by wide quasi-stationary lows often surrounded by one or more small mobile

142   lows. East to the Drake Passage the South Atlantic subtropical anticyclone extends southwards to the

143   Weddell sea, being this pattern almost symmetric with LWS. This cluster transports warm and moist

144   air over the Antarctic Peninsula often associated to precipitation in the area (van Loon 1967).

145   *Low over the Drake Passage (LDP)*

146         This cluster aggregates the lows over and west to the Drake Passage. These lows may have

147   both a zonal path crossing the Drake Passage to the east, or a meridian path either northwards or

148 southwards as a result of a blocking high. Blocking highs are suggested in the cluster center by a

149 slight ridge located over South Atlantic that sometimes couples with the Antarctic continental

150 anticyclone.

151 *Zonal over the Drake Passage (ZDP)*
152       This cluster is characterized by an intense westerly flow over the Drake Passage and Tierra

153 del Fuego with mobile cyclones moving eastwards at high latitudes along the Circumpolar Trough.

154 Those cyclones crosses from Bellingshausen Sea to Weddell Sea through the AP and may suffer a

155 variety of orographic processes on their paths (Mayes 1985).

156 *Ridge over the Antarctic Peninsula (RAP)*
157       This cluster presents a meridian circulation characterized by an anticyclonic ridge extending

158 southward from South America to the Drake Passage and the AP associated to the wavenumber-3

159 pattern in the region (van Loon and Jenne 1972). This ridge is flanked by two quasi-stationary wide

160 lows, which enhance the meridian circulation. Western low may be associated to a western

161 displacement of the ABSL.

162

163 ## b) Frequency of occurrence
164       The five atmospheric patterns present a similar frequency all ranging between 18 and 22 %

165 (Table 1). The most common pattern is ZDP with a frequency of 22.0% of days and the less common

166 is LWS with 18.4% of days. There is a notable variability in pattern frequencies between seasons.

167 For example, LAB shows an increase of frequency during the equinoxes, especially in the spring,

168 associated to the Semi-Annual Oscillation (SAO) when the wavenumber-3 pattern of the circumpolar

169 trough (one of the troughs located over Amundsen-Bellingshausen seas) contracts and deepens

170 southeastward (van Loon 1967; van den Broeke 1998, 2000). ZDP pattern also presents a noteworthy

171 frequency in spring when circumpolar trough is contracted and enhances the zonal winds around

172 Antarctica (Raphael 2004). In summer, when the polar jet slightly moves northwards, LDP pattern

173 becomes dominant. It is possible that the classification method associates systems north to the ABSL

174 inside LDP pattern. This would explain the low occurrence of LAB in summer and the shift to the

175 west of the LDP pattern in Figure 1. Autumn and winter present a more equilibrated distribution of

176 patterns, with a slight increase of LWS in winter associated to a larger density of cyclones near the

177 Flichner-Ronne ice shelf (Simmonds and Keay 2000) and a most western position of the ABSL

178 (Hosking et al. 2013).

179 ## c) Pattern persistence and sequences
180        Table 2 shows the pattern sequence between two consecutive days. The persistence is large

181 and correspond to the 64.7% of the days. The high values of persistence of atmospheric patterns

182 between two consecutive days indicates that the characteristic time for moving the different elements

183 that configure each cluster is longer than a day. The most common daily sequences of patterns are the

184 persistence of ZDP and LAB with 14.1% and 13.8% respectively. This is not surprising since they

185 are the two most common patterns in the region. Nonetheless, persistence is longer in LWS and LAB,

186 in which the mean number of consecutive persisting days is 3.2 and 3.1 respectively. RAP shows the

187 smallest value of both frequency of persistence (11.3 %) and mean number of consecutive days (2.5

188 days).

189       Non-persistence sequences correspond to the 35.3% of the days being each individual

190 sequence below 4%. The most common sequences are the change from RAP to LAB, LWS to RAP

191 and LAB to ZDP. It is not surprising that LWS to RAP (3.1%) and RAP to LAB (3.9%) along with

192 LAB to LDP (2.7%) and LDP to LWS (2.6%) sequences are so common. These four sequences (LWS

193 → RAP → LAB → LDP → LWS) constitute a chain where the synoptic waves move forward a

194 quarter-wavelength. In fact, the opposite sequences are in general very uncommon since they imply

195 a backward motion of the synoptic waves. Not surprisingly, there are no sequences between LWS

196 and LAB and vice versa since they imply a complete inversion of the ridges and lows in a day.

197       LAB to ZDP (3.1%) is also a common transition that occurs when the low over the

198 Bellingshausen Sea moves southeastward and crosses the Antarctic Peninsula. After this situation is

199 also common the change from ZDP to LWS (2.8%) probably due to the orographic cyclogenesis

200 leeside of Antarctic Peninsula (Mayes 1985). This chain (LAB → ZDP → LWS) may replace the

201 chain LAB → LDP → LWS when the flow is mainly zonal over the Drake Passage, and explains why

202 RAP to LAB has a larger frequency than the others. The complete cycle with these two chains is

203 outlined in Figure 4. The fact that all clusters are implicated into one or both transition chains may

204 explain the similar frequencies of all circulation patterns.

205 e) Climate variability and linear trends

206         Correlations between annual and seasonal occurrence of atmospheric patterns with SAM and

207 ENSO indices are shown in Table 3. Annual occurrence of most patterns significantly correlates with

208 SAM, with the only exception of RAP that show a weak correlation (*p-value* < 0.1). Seasonal

209 occurrences of patterns also show significant correlations with SAM with the exception of

210 correlations with RAP in autumn, winter and spring, and with LWS in summer. A positive SAM

211 increases the occurrence of ZDP and LAB since SAM is associated to the contraction and

212 intensification of the circumpolar westerly belt that strengths zonal conditions (Lefebvre et al. 2004;

213 Orr et al. 2008; Lubin et al. 2008) and it modulates the depth of the ABSL (Turner et al. 2013; Raphael

214 et al. 2016; Clem and Fogt 2013). These two patterns contribute to bring mild air to Antarctic

215 Peninsula. By contrast, positive SAM reduces the occurrence of LDP and LWS. SAM – LDP

216 anticorrelation is consistent with other studies that show a reduction of the number of cyclones

217 between 50º-60º S due to the poleward shift of their path during positive SAM conditions (Reboita et

218 al. 2015).

219         ENSO has much lower influence in the atmospheric patterns over the AP region than SAM.

220 Yet, there is a significant correlation between El Niño 3.4 SST anomalies and annual occurrences of

221 LAB and LWS. At seasonal scale, El Niño 3.4 correlates with LAB in spring, summer and autumn.

222 Through a tropospheric wave train, the cold (warm) phase of ENSO related to La Niña (El Niño)

223 strengths (weakens) the ABSL (Trenberth et al. 2002; Genthon and Cosme 2003), especially in spring

224 when the correlations between ENSO and temperatures in the AP are strongest (Clem and Fogt 2013;

225 Clem et al. 2016). El Niño 3.4 also correlates with LWS in winter and spring agreeing with the

226 increase of the cyclonic density east to the AP during the positive phase of ENSO (Reboita et al.

227 2015, in their figure 5). It is worth to note that the correlations between ENSO or SAM and LAB

228 occurrence are in agreement with the correlation between those teleconnections and central pressure

229 of ABSL calculated by Hosking et al. (2013, in their Table 2).

230    Related to stratospheric ozone depletion and greenhouse gas increases, SAM has shown a

231    positive trend since 1958 (Thompson and Solomon 2002; Marshall et al. 2004) specially in summer

232    and autumn. This increase in positive SAM conditions has contributed to an increase of the

233    temperature in the AP during the last 60 years (Marshall 2007) by intensifying cyclonic conditions in

234    high latitudes (Thompson and Solomon 2002), enhancing lee-side foehn winds on the eastern

235    Peninsula (Orr et al. 2008) and increasing meridional winds by amplifying the ABSL (Fogt et al.

236    2011, 2012; Turner et al. 2013; Hosking et al. 2013). Therefore, it is expected to find a change in the

237    patterns occurrence associated to the increase of the SAM.

238    Table 4 shows the linear temporal evolution of frequency for each atmospheric pattern

239    between 1979 and 2016. The only significant trends found at >95% significance are an increase of

240    LWS in summer and an increase of LAB in autumn and all-year round. Weak trends are also observed

241    in summer to increase ZDP and decrease LDP. The increase of LAB occurrences for both in all-year

242    round and autumn may be associated to the increase of SAM (Hosking et al. 2013; Raphael et al.

243    2016). Increase of zonal conditions in summer may enhance lee cyclogenesis around Antarctic

244    Peninsula (Mayes 1985; Orr et al. 2008) that would explain the increase of LWS occurrence in DJF.

## 4. Application to Livingston Island

246    South Shetland Islands, as well as the northern edge of the Antarctic Peninsula, are located

247    near the center of the study area. Thus, it is expected that Livingston Ice Cap response may be

248    influenced by the occurrence of the different circulation patterns advecting different air masses. This

249    effect may be especially important in summer, when the ice caps are more sensitive to temperature

250    changes. Indeed, Jonsell et al. (2012) have shown that Livingston Ice Cap surface mass balance is

251    very sensitive to small changes in temperature during the melt season, calculating that 0.5 ºC increase

252    results in 56% higher melt rates. They also noticed that high peaks in melt coincide with moist and

253    warm fluxes arising from NW. This suggests that LAB pattern may produce those peaks in melt.

254    Figure 5 shows the bivariate distribution of daily temperature and moisture anomalies with

255    respect of the monthly mean for each circulation pattern at JCI AWS in Livingston Island calculated

using a kernel density estimation. As expected, LAB is prone to transport warm and moist air to the Shetland Islands from south-east Pacific while LWS and RAP advects cold and dry air from the continent. Therefore, those two patterns may largely affect the Livingston Ice Cap surface balance being mainly negative during LAB conditions and stabilizing during LWS or RAP conditions. Both, ZDP and LDP presents mild temperatures, but whereas ZDP bears mainly moist air, LDP presents a dual behavior. LDP shows two peaks in the density function with different moisture. This behavior may be produced by the different air advection depending on the position of the low respect to the island. When the low is located west to Livingston, warm moist air is transported to JCI. When the low crosses to east, the air becomes cooler and dryer. Nonetheless, those relationships and the real effect into the cryosphere should be further explored.

Figure 6 shows the distribution of daily precipitation anomalies with respect the monthly mean in JCI AWS for each circulation pattern. Days with LAB pattern present more positive precipitation anomalies. ZDP in general shows positive precipitation anomalies although it also presents many days with dry anomalies. Most of the dry days were classified as RAP, LWS or LDP. It is worth to note that dichotomy presented by LDP for moisture is also conspicuous for precipitation, with two relative peaks in the density function for both positive and negative precipitation anomalies. Indeed, the largest anomalies of precipitation in JCI (the right tail of the plot) are not produced by LAB but for both LDP and ZDP patterns. This indicates that LAB does not determine the largest precipitation episodes but light drizzle events. Those results should be carefully considered due to the limitations of the rain gauges when snowfall is collected.

## 5. Conclusions

Five synoptic pressure patterns have been computed from ERA Interim reanalysis using cluster analysis in the AP region (45ºS 75ºS 20ºW 120ºW). All five types present a similar frequency during the year but they manifest a large seasonal variability as a result of changing climatological structures as SAO, polar jet movement, etc. Transition between synoptic patterns tends to follow a cycle where synoptic waves move eastwards a quarter-wavelength. This cycle has two modes, one

282  with larger latitudinal amplitude and meridional circulation, and another one with enhanced zonal

283  circulation. Climate modes of variability as ENSO or SAM have a large influence in the frequency

284  of patterns over the AP region. For example, as other studies suggest (i. e. Clem and Fogt 2013), cold

285  phase of the ENSO in spring is associated with an enhanced ABSL and a reduction of the Weddell

286  Low. All synoptic patterns show a larger correlation with SAM than with ENSO. During the positive

287  SAM, the ABSL becomes strengthened and zonal circulation increases. By contrast, lows over Drake

288  Passage and Weddell Sea prevails during negative SAM. Indeed, increase of LAB conditions may be

289  explained by the increase of SAM as a result of stratospheric ozone depletion and greenhouse gas

290  increases (Thompson and Solomon 2002; Marshall et al. 2004).

291  As pointed out by Cohen et al. (2013), there exists many potential uses to the synoptic patterns.

292  In this paper, we conducted a cursory analysis to explore the possibility of determining the air mass

293  characteristics associated to each pattern that may affect the surface mass balance of the ice cap on

294  Livingston Island. Synoptic patterns have been shown to be a useful tool to study air mass advections

295  that may affect the surface mass balance of ice caps and ice sheets in the periphery of Antarctica.

296  Different patterns may carry different air masses. For example, LAB transports a warm and moist air

297  and often slight precipitation to the South Shetland Islands while LWS is associated with dry and cold

298  air. We suggest that changing of synoptic types occurrence, especially in summer may dramatically

299  affect to the stability of glaciers and island ice caps. Future work will further explore the effects in

300  the cryosphere with changing synoptic types.

# References

Arthur, D., and S. Vassilvitskii, 2007: k-means++: the advantages of careful seeding. *Proceedings of the eighteenth annual ACM-SIAM symposium on Discrete algorithms*, Philadelphia, Society for Industrial and Applied Mathematics, 1027–1025.

Bamston, A. G., M. Chelliah, and S. B. Goldenberg, 1997: Documentation of a highly ENSO‐related sst region in the equatorial pacific: Research note. *Atmosphere-Ocean*, **35**, 367–383, doi:10.1080/07055900.1997.9649597.

Bañon, M., and F. Vasallo, 2015: *Aemet en la Antártida. Climatología y meteorología sinóptica en las estaciones meteorológicas en las estaciones meteorológicas españolas en la Antártida*. AEMET, Min. Madrid, 150 pp.

Bliss, A., R. Hock, and J. G. Cogley, 2013: A new inventory of mountain glaciers and ice caps for the Antarctic periphery. *Ann. Glaciol.*, **54**, 191–199, doi:10.3189/2013AoG63A377.

Bracegirdle, T. J., and G. J. Marshall, 2012: The reliability of antarctic tropospheric pressure and temperature in the latest global reanalyses. *J. Clim.*, **25**, 7138–7146, doi:10.1175/JCLI-D-11-00685.1.

van den Broeke, M. R., 1998: The semi-annual oscillation and Antarctic climate. Part I : influence on near surface temperatures (1957-79). *Antarct. Sci.*, **10**, 175–183, doi:10.1017/S095410209800025X.

——, 2000: The semi-annual oscillation and antarctic climate. Part 3: The role of near-surface wind speed and cloudiness. *Int. J. Climatol.*, **20**, 117–130, doi:10.1002/(SICI)1097-0088(200002)20:2<117::AID-JOC481>3.0.CO;2-B.

——, and N. P. M. van Lipzig, 2003: Response of wintertime Antarctic temperatures to the antarctic oscillation: Results of a regional climate model. *Antarctic Peninsula Climate Variablity: Historical and Paleoenvironmental Perspectives*, Vol. 79 of, American Geophysical Union, 43–58.

——, and N. P. M. van Lipzig, 2004: Changes in Antarctic temperature, wind and precipitation in

response to the Antarctic Oscillation. *Ann. Glaciol.*, **39**, 119–126, doi:10.3189/172756404781814654.

Carleton, A. M., 2003: Atmospheric teleconnections involving the Southern Ocean. *J. Geophys. Res.*, **108**, 8080, doi:10.1029/2000JC000379.

Carrasco, J. F., 2013: Decadal Changes in the Near-Surface Air Temperature in the Western Side of the Antarctic Peninsula. *Atmos. Clim. Sci.*, **3**, 275–281, doi:10.4236/acs.2013.33029.

Clem, K. R., and R. L. Fogt, 2013: Varying roles of ENSO and SAM on the Antarctic Peninsula climate in austral spring. *J. Geophys. Res. Atmos.*, **118**, 11,481-11,492, doi:10.1002/jgrd.50860.

——, J. A. Renwick, J. McGregor, and R. L. Fogt, 2016: The relative influence of ENSO and SAM on Antarctic Peninsula climate. *J. Geophys. Res. Atmos.*, **121**, 9324–9341, doi:10.1002/2016JD025305.

Cohen, L., S. Dea, and J. Renwick, 2013: Synoptic weather types for the ross sea region, Antarctica. *J. Clim.*, **26**, 636–649, doi:10.1175/JCLI-D-11-00690.1.

Dee, D. P., and Coauthors, 2011: The ERA-Interim reanalysis: Configuration and performance of the data assimilation system. *Q. J. R. Meteorol. Soc.*, **137**, 553–597, doi:10.1002/qj.828.

Fogt, R. L., and D. H. Bromwich, 2006: Decadal variability of the ENSO teleconnection to the high-latitude south pacific governed by coupling with the Southern Annular mode. *J. Clim.*, **19**, 979–997, doi:10.1175/JCLI3671.1.

——, ——, and K. M. Hines, 2011: Understanding the SAM influence on the South Pacific ENSO teleconnection. *Clim. Dyn.*, **36**, 1555–1576, doi:10.1007/s00382-010-0905-0.

——, A. J. Wovrosh, R. A. Langen, and I. Simmonds, 2012: The characteristic variability and connection to the underlying synoptic activity of the Amundsen-Bellingshausen Seas Low. *J. Geophys. Res. Atmos.*, **117**, D07111, doi:10.1029/2011JD017337.

Gardner, A. S., and Coauthors, 2013: A reconciled estimate of glacier contributions to sea level rise: 2003 to 2009. *Science*, **340**, 852–857, doi:10.1126/science.1234532.

Genthon, C., and E. Cosme, 2003: Intermittent signature of ENSO in west-Antarctic precipitation. *Geophys. Res. Lett.*, **30**, 2081, doi:10.1029/2003GL018280.

Govorukha, L. S., and V. Y. Timofeyev, 2002: Synoptic circulation types of Antarctic Peninsula and adjacent South Ocean regions and connected phenomena. *Probl. Klimatologii Polarn.*, **10**, 159–178.

Guijarro, J. A., 2017: Daily series homogenization and gridding with Climatol v.3. *Proceedings of the 9th Seminar for homogenization and quality control in climatological databases and 4th conference on spatial interpolation techniques in climatology and meteorology*, Budapest, 3-7 de Abril, (in press).

Hock, R., M. De Woul, V. Radic, and M. Dyurgerov, 2009: Mountain glaciers and ice caps around Antarctica make a large sea-level rise contribution. *Geophys. Res. Lett.*, **36**, L07501, doi:10.1029/2008GL037020.

Hosking, J. S., A. Orr, G. J. Marshall, J. Turner, and T. Phillips, 2013: The influence of the amundsen-bellingshausen seas low on the climate of West Antarctica and its representation in coupled climate model simulations. *J. Clim.*, **26**, 6633–6648, doi:10.1175/JCLI-D-12-00813.1.

Houssos, E. E., C. J. Lolis, and A. Bartzokas, 2008: Advances in Geosciences Atmospheric circulation patterns associated with extreme precipitation amounts in Greece. *Adv. Geosci.*, **17**, 5–11.

IPCC, 2013: *Climate Change 2013: The Physical Science Basis. Contribution of Working Group I to the Fifth Assessment Report of the Intergovernmental Panel on Climate Change*. 1535 pp.

Jonsell, U. Y., F. J. Navarro, M. Bañón, J. J. Lapazaran, and J. Otero, 2012: Sensitivity of a distributed temperature-radiation index melt model based on AWS observations and surface energy balance fluxes, Hurd Peninsula glaciers, Livingston Island, Antarctica. *Cryosphere*, **6**, 539–552, doi:10.5194/tc-6-539-2012.

Kejna, M., 1993: Types of Atmospheric Circulation in the Region of H. Arctowski Station (South Shetland Islands) in the years 1986-1989. *XX Polar Symposium*, 369–378.

Lana, A., J. Campins, A. Genovés, and A. Jansà, 2007: Atmospheric patterns for heavy rain events in the Balearic Islands. *Adv. Geosci.*, **12**, 27–32, doi:10.5194/adgeo-12-27-2007.

Lefebvre, W., H. Goosse, R. Timmermann, and T. Fichefet, 2004: Influence of the Southern Annular Mode on the sea ice - Ocean system. *J. Geophys. Res. C Ocean.*, **109**, 1–12, doi:10.1029/2004JC002403.

van Loon, H., 1967: The Half-Yearly Oscillations in Middle and High Southern Latitudes and the Coreless Winter. *J. Atmos. Sci.*, **24**, 472–486, doi:10.1175/1520-0469(1967)024<0472:THYOIM>2.0.CO;2.

——, and R. L. Jenne, 1972: The zonal harmonic standing waves in the southern hemisphere. *J. Geophys. Res.*, **77**, 992, doi:10.1029/JC077i006p00992.

Lubin, D., R. A. Wittenmyer, D. H. Bromwich, and G. J. Marshall, 2008: Antarctic Peninsula mesoscale cyclone variability and climatic impacts influenced by the SAM. *Geophys. Res. Lett.*, **35**, L02808, doi:10.1029/2007GL032170.

Ludescher, J., A. Bunde, C. L. E. Franzke, and H. J. Schellnhuber, 2016: Long-term persistence enhances uncertainty about anthropogenic warming of Antarctica. *Clim. Dyn.*, **46**, 263–271, doi:10.1007/s00382-015-2582-5.

Marshall, G. J., 2003: Trends in the Southern Annular Mode from observations and reanalyses. *J. Clim.*, **16**, doi:10.1175/1520-0442(2003)016<4134:TITSAM>2.0.CO;2.

Marshall, G. J., 2007: Half-century seasonal relationships between the Southern Annular Mode and Antarctic temperatures. *Int. J. Climatol.*, **27**, 373–383, doi:10.1002/joc.1407.

——, P. A. Stott, J. Turner, W. M. Connolley, J. C. King, and T. A. Lachlan‐Cope, 2004: Causes of exceptional atmospheric circulation changes in the Southern Hemisphere. *Geophys. Res. Lett.*, **31**, L14205, doi:10.1029/2004GL019952.

——, A. Orr, N. P. M. van Lipzig, and J. C. King, 2006: The impact of a changing Southern Hemisphere Annular Mode on Antarctic Peninsula summer temperatures. *J. Clim.*, **19**, 5388–5404, doi:10.1175/JCLI3844.1.

Mayes, P. R., 1985: Secular variations in cyclone frequencies near the Drake Passage, southwest Atlantic. *J. Geophys. Res.*, **90**, 5829–5839, doi:10.1029/JD090iD03p05829.

Oliva, M., F. Navarro, F. Hrbáček, A. Hernández, D. Nývlt, P. Pereira, J. Ruiz-Fernández, and R. Trigo, 2017: Recent regional climate cooling on the Antarctic Peninsula and associated impacts on the cryosphere. *Sci. Total Environ.*, **580**, 210–223, doi:10.1016/j.scitotenv.2016.12.030.

Orr, A., G. J. Marshall, J. C. R. Hunt, J. Sommeria, C.-G. Wang, N. P. M. van Lipzig, D. Cresswell, and J. C. King, 2008: Characteristics of Summer Airflow over the Antarctic Peninsula in Response to Recent Strengthening of Westerly Circumpolar Winds. *J. Atmos. Sci.*, **65**, 1396–1413, doi:10.1175/2007JAS2498.1.

Radić, V., and R. Hock, 2010: Regional and global volumes of glaciers derived from statistical upscaling of glacier inventory data. *J. Geophys. Res. Earth Surf.*, **115**, F01010, doi:10.1029/2009JF001373.

——, and ——, 2011: Regionally differentiated contribution of mountain glaciers and ice caps to future sea-level rise. *Nat. Geosci.*, **4**, 91–94, doi:10.1038/ngeo1052.

Raphael, M. N., 2004: A zonal wave 3 index for the Southern Hemisphere. *Geophys. Res. Lett.*, **31**, 1–4, doi:10.1029/2004GL020365.

——, and Coauthors, 2016: The Amundsen sea low: Variability, change, and impact on Antarctic climate. *Bull. Am. Meteorol. Soc.*, **97**, 111–121, doi:10.1175/BAMS-D-14-00018.1.

Rayner, N. A., D. E. Parker, E. B. Horton, C. K. Folland, L. V. Alexander, D. P. Rowell, E. C. Kent, and A. Kaplan, 2003: Global analyses of sea surface temperature, sea ice, and night marine air temperature since the late nineteenth century. *J. Geophys. Res.*, **108**, 4407, doi:10.1029/2002JD002670.

Reboita, M. S., R. P. da Rocha, T. Ambrizzi, and C. D. Gouveia, 2015: Trend and teleconnection patterns in the climatology of extratropical cyclones over the Southern Hemisphere. *Clim. Dyn.*, **45**, 1929–1944, doi:10.1007/s00382-014-2447-3.

Simmonds, I., and K. Keay, 2000: Mean southern hemisphere extratropical cyclone behavior in the 40-year NCEP-NCAR reanalysis. *J. Clim.*, **13**, 873–885, doi:10.1175/1520-0442(2000)013<0873:MSHECB>2.0.CO;2.

Thompson, D. W. J., and S. Solomon, 2002: Interpretation of recent Southern Hemisphere climate change. *Science*, **296**, 895–899, doi:10.1126/science.1069270.

Trenberth, K. E., J. M. Caron, D. P. Stepaniak, and S. Worley, 2002: Evolution of El Niño–Southern Oscillation and global atmospheric surface temperatures. *J. Geophys. Res.*, **107**, 4065, doi:10.1029/2000JD000298.

Turner, J., G. J. Marshall, and T. A. Lachlan-Cope, 1998: Analysis of synoptic-scale low pressure systems within the Antarctic Peninsula sector of the circumpolar trough. *Int. J. Climatol.*, **18**, 253–280, doi:10.1002/(SICI)1097-0088(19980315)18:3<253::AID-JOC248>3.0.CO;2-3.

——, T. Phillips, J. S. Hosking, G. J. Marshall, and A. Orr, 2013: The amundsen sea low. *Int. J. Climatol.*, **33**, 1818–1829, doi:10.1002/joc.3558.

——, and Coauthors, 2016: Absence of 21st century warming on Antarctic Peninsula consistent with natural variability. *Nature*, **535**, 411–415, doi:10.1038/nature18645.

Vaughan, D. G., and Coauthors, 2003: Recent rapid regional climate warming on the Antarctic Peninsula. *Clim. Change*, **60**, 243–274, doi:10.1023/A:1026021217991.

Table 1. Seasonal and annual frequency (%) of each synoptic pattern during the period comprised between 1979 and 2016.

|       | LWS  | LAB  | LDP  | ZDP  | RAP  |
|-------|------|------|------|------|------|
| DJF   | 16.5 | 16.0 | 28.9 | 21.4 | 17.1 |
| MAM   | 17.4 | 20.6 | 20.8 | 19.4 | 21.8 |
| JJA   | 23.0 | 19.3 | 17.5 | 19.5 | 20.6 |
| SON   | 16.5 | 26.0 | 13.7 | 27.8 | 15.9 |
| Total | 18.4 | 20.5 | 20.2 | 22.0 | 18.9 |

Table 2. Frequency (%) of pattern sequences between two consecutive days during the period comprised between 1979 and 2016. Values in the diagonal (in bold) show the daily persistence for each synoptic pattern. Values in brackets show the mean consecutive days in which each pattern persist. Values in parenthesis show the frequency considering only the changing sequences, that is, when the persistence is removed.

|              |      | To pattern |            |            |            |            |
|--------------|------|------------|------------|------------|------------|------------|
|              |      | LWS        | LAB        | LDP        | ZDP        | RAP        |
|              | LWS  | **12.6 [3.2]** | 0.0 (0.0)  | 0.9 (2.5)  | 1.8 (5.1)  | 3.1 (8.8)  |
| **From**     | LAB  | 0.0 (0.0)  | **13.8 [3.1]** | 2.7 (7.6)  | 3.1 (8.8)  | 0.9 (2.5)  |
| **pattern**  | LDP  | 2.6 (7.4)  | 1.0 (2.8)  | **12.9 [2.8]** | 2.0 (5.7)  | 1.8 (5.1)  |
|              | ZDP  | 2.8 (7.9)  | 1.8 (5.1)  | 1.5 (4.2)  | **14.1 [2.8]** | 1.9 (5.4)  |
|              | RAP  | 0.4 (1.1)  | 3.9 (11.0) | 2.2 (6.2)  | 1.0 (2.8)  | **11.3 [2.5]** |

Table 3. Correlations and statistical signification between seasonal occurrence of synoptic patterns and SAM and El Niño 3.4 indices during the period comprised between 1979 and 2016. *p*-values are indicated in parenthesis. Bolded values indicate statistically significant correlations at 95% confidence.

|       | SAM            |                |                |                |                |
|-------|----------------|----------------|----------------|----------------|----------------|
|       | Annual         | DJF            | MAM            | JJA            | SON            |
| LWS   | **-0.44 (0.006)** | -0.07 (0.674)  | **-0.62 (0.000)** | **-0.39 (0.010)** | **-0.45 (0.005)** |
| LAB   | **0.56 (0.000)**  | **0.32 (0.048)**  | **0.57 (0.000)**  | **0.57 (0.000)**  | **0.54 (0.000)**  |
| LDP   | **-0.53 (0.001)** | **-0.67 (0.000)** | **-0.41 (0.010)** | **-0.37 (0.020)** | **-0.71 (0.000)** |
| ZDP   | **0.49 (0.002)**  | **0.80 (0.000)**  | **0.64 (0.000)**  | **0.37 (0.023)**  | **0.42 (0.008)**  |
| RAP   | -0.28 (0.094)  | **-0.40 (0.011)** | -0.15 (0.379)  | -0.10 (0.538)  | -0.29 (0.080)  |
|       | El Niño 3.4    |                |                |                |                |
|       | Annual         | DJF            | MAM            | JJA            | SON            |
| LWS   | **0.38 (0.017)**  | 0.30 (0.062)   | 0.16 (0.350)   | **0.33 (0.043)**  | **0.61 (0.000)**  |
| LAB   | **-0.39 (0.015)** | **-0.38 (0.018)** | **-0.34 (0.038)** | -0.22 (0.183)  | **-0.52 (0.001)** |
| LDP   | 0.12 (0.452)   | 0.19 (0.257)   | 0.06 (0.738)   | -0.14 (0.403)  | 0.20 (0.219)   |
| ZDP   | -0.20 (0.219)  | -0.16 (0.322)  | 0.02 (0.908)   | 0.05 (0.789)   | -0.01 (0.939)  |
| RAP   | 0.01 (0.941)   | -0.09 (0.579)  | 0.10 (0.559)   | -0.12 (0.468)  | -0.07 (0.684)  |

Table 4. Annual and seasonal linear trends of synoptic pattern frequencies during the period comprised between 1979 and 2016. *p*-values are indicated in parenthesis. Bolded values indicate statistically significant trends at 95% confidence.

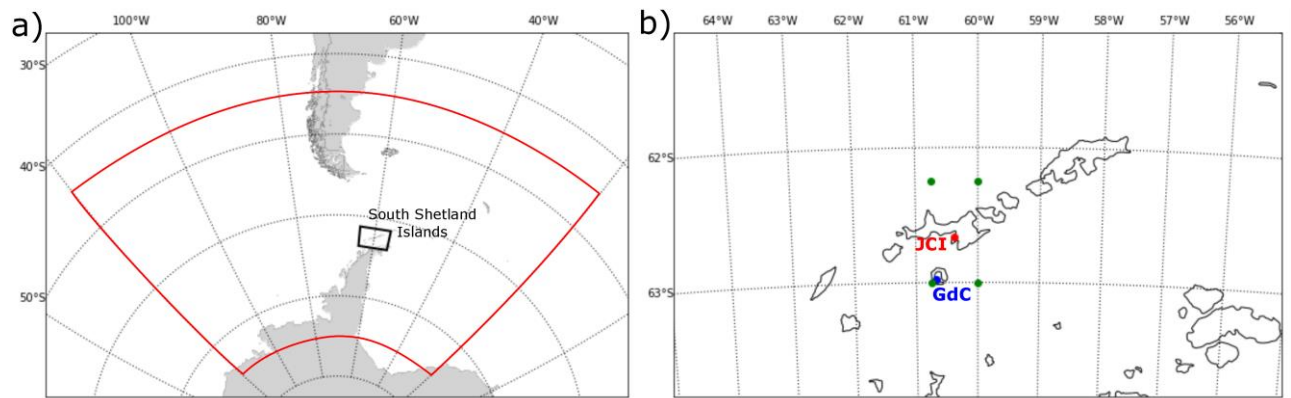|  | Annual | DJF | MAM | JJA | SON |
|---|---|---|---|---|---|
| LWS | -0.82 (0.329) | **2.72 (0.025)** | -2.43 (0.096) | -2.46 (0.114) | -0.42 (0.754) |
| LAB | **1.56 (0.047)** | 0.40 (0.678) | **3.15 (0.009)** | -0.22 (0.868) | 3.10 (0.086) |
| LDP | -0.79 (0.196) | -3.32 (0.065) | -0.24 (0.817) | 1.18 (0.225) | 0.09 (0.937) |
| ZDP | 0.63 (0.409) | 3.11 (0.054) | 0.35 (0.778) | 0.80 (0.431) | -1.33 (0.409) |
| RAP | -0.58 (0.210) | -1.20 (0.109) | -0.84 (0.470) | 0.69 (0.557) | -1.16 (0.194) |

Figure 1. a) Map of the geographic area showing the area used to perform the cluster analysis (red) and the area depicted in b (black). b) South Shetland Islands region indicating JCI station (in red), GdC station (in blue) and the four ERA Interim reanalysis points used to homogenize the data (in green).
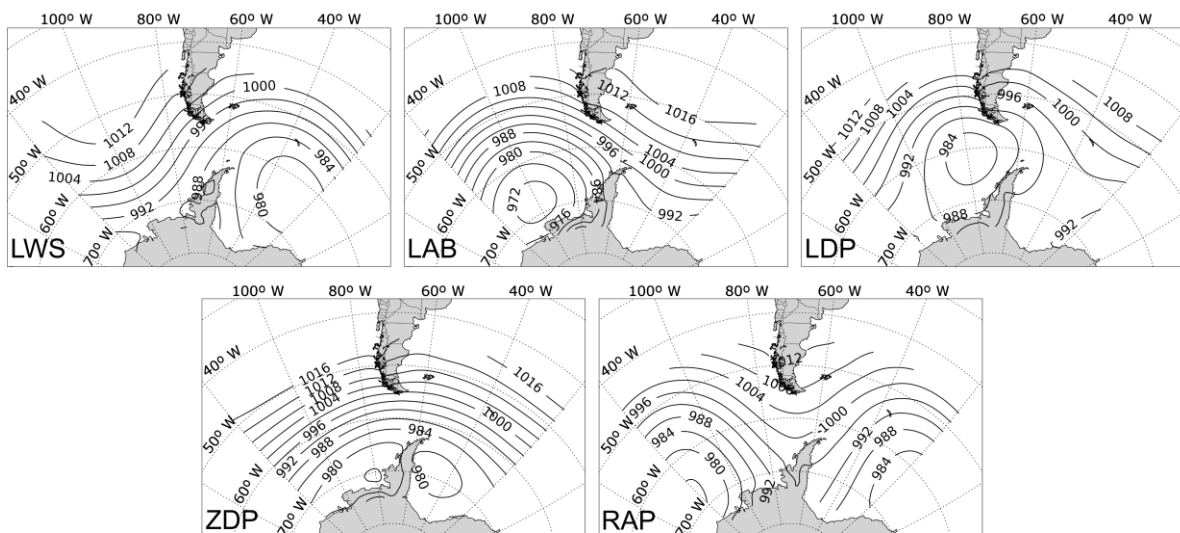
Figure 2. Synoptic patterns (cluster centroids) calculated using ERA Interim reanalysis for the AP region over the period comprised between 1979 and 2016.
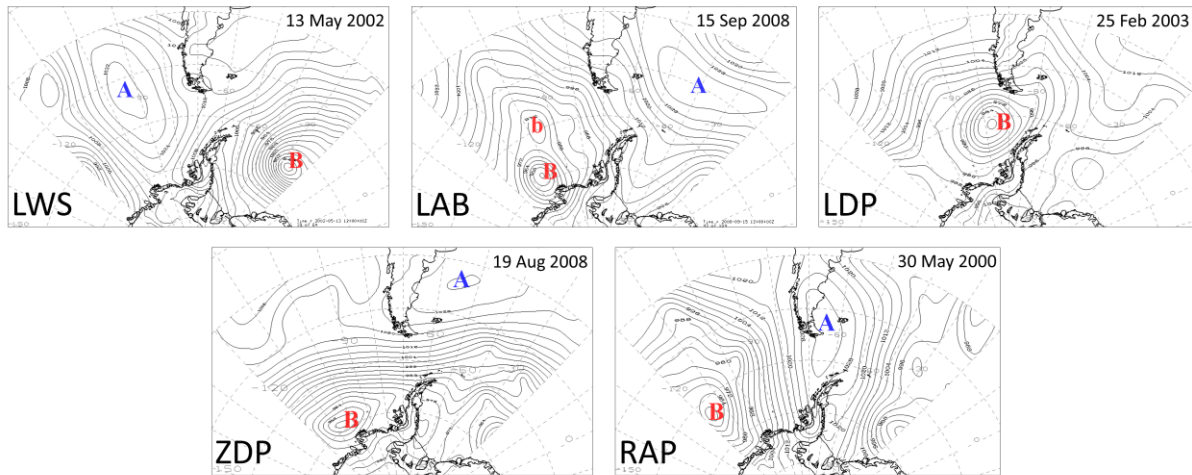
Figure 3. Examples of ERA Interim synoptic analysis in the AP for each cluster. LWS: 13 May 2002; LAB: 15 Sep 2008; LDP: 25 Feb 2003; ZDP: 19 Aug 2008; RAP: 30 May 2000.

Figure 4. Scheme of the most common transitions between synoptic patterns in the AP. The width of the arrows is proportional to the frequency of each transition.

Figure 5. Bivariate density function of daily temperature and relative humidity anomalies respect to the monthly mean for each synoptic pattern at JCI AWS. The period considered is comprised between 2005 and 2016. Each pattern displays a different scale to better visualize the peak of the function (shaded).

Figure 6. Density function of daily precipitation anomalies respect to the monthly mean for each synoptic pattern at JCI AWS. The period considered is comprised between 2005 and 2016.

Figure 1. a) Map of the geographic area showing the area used to perform the cluster analysis (red) and the area depicted in b (black). b) South Shetland Islands region indicating JCI station (in red), GdC station (in blue) and the four ERA Interim reanalysis points used to homogenize the data (in green).



Figure 2. Synoptic patterns (cluster centroids) calculated using ERA Interim reanalysis for the AP region over the period comprised between 1979 and 2016.

Figure 3. Examples of ERA Interim synoptic analysis in the AP for each cluster. LWS: 13 May 2002; LAB: 15 Sep 2008; LDP: 25 Feb 2003; ZDP: 19 Aug 2008; RAP: 30 May 2000.
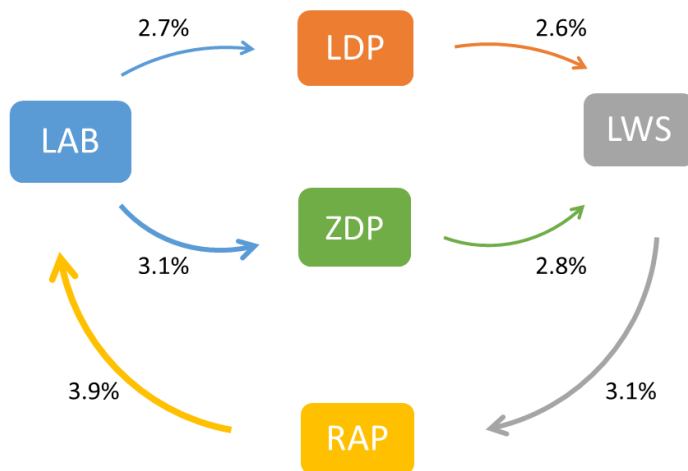


Figure 4. Scheme of the most common transitions between synoptic patterns in the AP. The width of the arrows is proportional to the frequency of each transition.
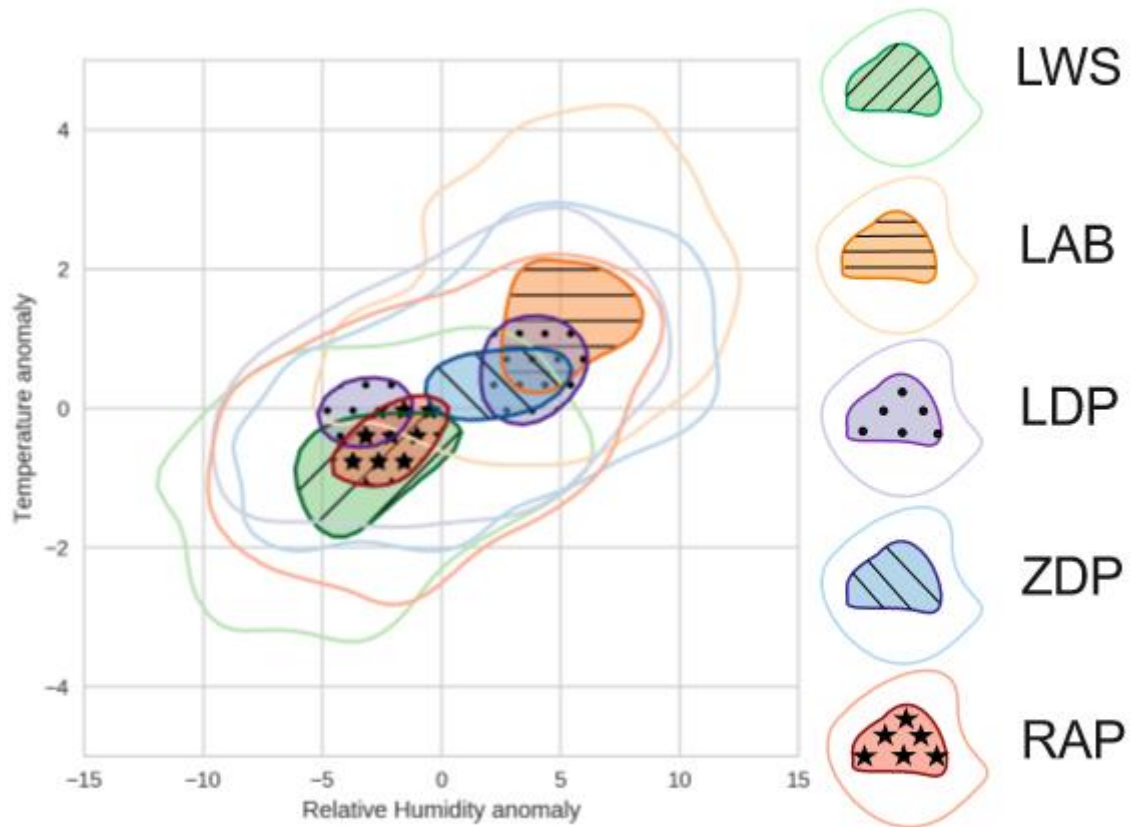
Figure 5. Bivariate density function of daily temperature and relative humidity anomalies respect to the monthly mean for each synoptic pattern at JCI AWS. The period considered is comprised between 2005 and 2016. Each pattern displays a different scale to better visualize the peak of the function (shaded).
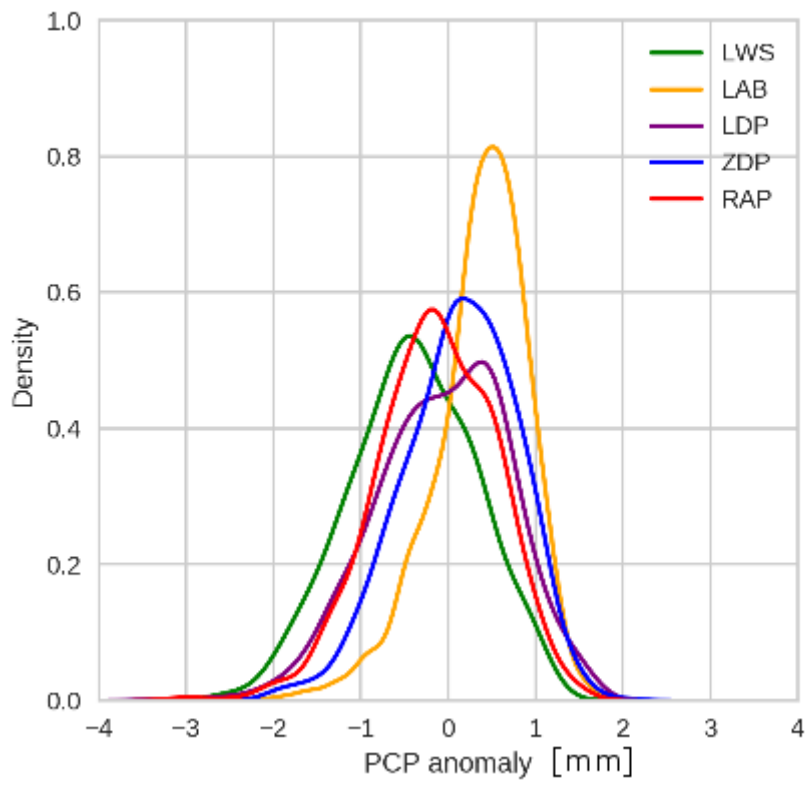
Figure 6. Density function of daily precipitation anomalies respect to the monthly mean for each synoptic pattern at JCI AWS. The period considered is comprised between 2005 and 2016.